

GYROSCOPIC FORCE MEASURING SYSTEM

S. Kurosu, M. Kasahara and K. Kodama

Oyama National College of Technology
771 Nakakuki, Oyama-city, 323-0806 Japan

Abstract. This paper concerns the development of an entirely new sensor (called Gyroscopic Force Measuring System, or simply called GFMS) for measuring a force vectorially. The principle and the dynamical characteristics of the GFMS for measuring a force vector are analyzed theoretically. Two auxiliary turntables (driven by servomechanisms) are installed around the gyroscope, in which turntables rotate to follow some angles of incidence of a force vector. Some unfavorable errors caused by various factors are analyzed. A compensation method is proposed as a device both for accurate force measurement and disturbance suppression. The feasibility of the proposed GFMS is confirmed by numerical simulations.

Keywords: Force measurement, Gyroscope, Gyroscopic force measuring system

1 INTRODUCTION

Two decades ago, a class of weight measuring device known as Gyroscopic Force Measuring System (simply called GFMS) has emerged in Germany as a highly precise replacement for existing weighing scales for centuries [1]. This GFMS provides precise, direct digital output proportional to single-axis (scalar) force applied. Its operation is unaffected by rotational friction, which is detected and counteracted by the use of a torque motor. The action of GFMS is inherently linear, hysteresis and drift free. Its dependability has been proved over the last two decades at numerous installations [3,4,5]. The GFMS constructed in our work [2] offered a repeatable accuracy up to 1/15,000 for force ranging from 0 to 150 N. The results of this work are directly applicable to measurement of a vectorial force.

The establishment of a force measurement in three-dimensional space will be indispensable for scientific and industrial fields in the near future. This paper explores the possible applicability of the GFMS to the vectorial measurement of a force. This analysis allows us to design the GFMS with suitable parameters to offer a reasonable accuracy. The total performance designed in this study is demonstrated by numerical simulations. Some theoretical errors associated with a new sensor are highlighted.

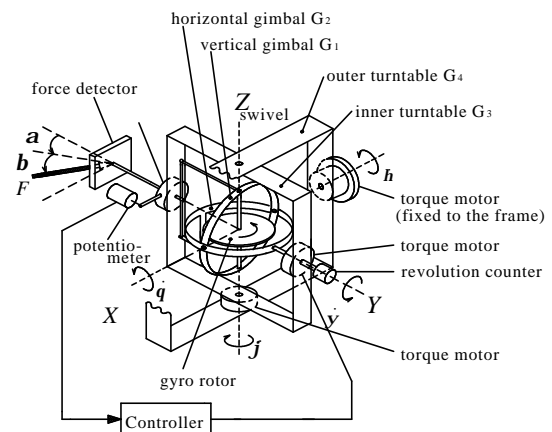


Figure 1. Construction model of GFMS

2 EQUATIONS OF MOTION

2.1 Construction and principles

Fig. 1 shows the GFMS to be considered in this paper. The gyro-rotor, which is mounted in gimbals with its axis vertical, spins at a constant speed and strictly rotate the horizontal axis OY. The vertical gimbal G_1 , which supports the rotor, is free to rotate relative to the horizontal gimbal G_2 about OX, while the horizontal gimbal G_2 is free to rotate relative to the inner turntable G_3 about OY. The G_2 supports one end of a pivoted lever vertically. The other end of this lever mounts on the G_1 at one end of the spin-axis of the rotor. The inner turntable G_3 and the outer turntable G_4 , which support the gyroscope, are free to rotate relative to the G_4 and the frame about OZ and OX, respectively.

The force to be measured acts vectorially on the center of the lever through a swivel and therefore applies a horizontal component force on one end of the spin-axis of rotor at unknown angles of incidence \acute{a} and \hat{a} . The best estimated angles \acute{a} and \hat{a} could be easily defined as estimates for which

the force F will be at maximum value. The servomechanisms of the G_3 and G_4 serve this purpose even better because the algorithm can be easily programmed. This principle of the GFMS is somewhat, similar to that of a well-known weathercock. This is why, in the GFMS, the force detector's aspect in space perpendicular to the direction of the object force is of dominant importance. The torque generated by the force applied causes the rotor in its gimbals to turn about OY and the rate of primary precession $\mathbf{w} = \dot{\mathbf{y}}$ is directly proportional to the force F applied.

This GMFS has some crucial disadvantages. First, the rotor is subjected to a precession $\dot{\mathbf{u}}$ about OY , which results in gyroscopic reaction torques about OZ and OX . These torques produce sustained oscillations on the G_3 and G_4 as disturbance inputs. Thus, in order to reduce the effects of the disturbance, we must present a compensation method over the frequency band of the disturbances. Second, the angles of incidence of a force applied are unknown to us. Thus estimation errors for the angles will be serious to the GMFS.

2.2 Analytical description

The spin-axis of the rotor is defined by four rotations: namely \mathbf{h} about OX , \mathbf{j} about Oz_4 , \mathbf{y} about Oy_3 , and \mathbf{e} about Ox_2 . Euler's dynamical equations for the motion of a rigid body about a fixed point lead to the general motion of the GFMS. To consider now the operation of the GFMS as in Fig. 1 with the spin-axis OZ vertical and to point the output axis OY toward the direction of the force F , we suppose that the force vector F which acts on the force detector can be defined by two rotations required to move them from coincidence with $O-XYZ$ to their final position, namely \mathbf{a} about OX and \mathbf{b} about OZ' . The equations of motion of this system can be described as follows:

$$\left. \begin{aligned} A\ddot{\mathbf{q}} + c_1\dot{\mathbf{q}} + H_0\dot{\mathbf{y}} &= T_{1x1}, & B\ddot{\mathbf{y}} + c_2\dot{\mathbf{y}} - H_0\dot{\mathbf{q}} &= T_{2y2} \\ (C + D_1 \cos^2 \mathbf{y} + D_2 \sin^2 \mathbf{y})\ddot{\mathbf{j}} + \{c_3 + (D_2 - D_1)\dot{\mathbf{y}} \sin \mathbf{y} \cos \mathbf{y}\}\dot{\mathbf{j}} &= -T_{1x1} \sin \mathbf{y} - T_{3z3} \\ (E + F_1 \cos^2 \mathbf{j} + F_2 \sin^2 \mathbf{j})\ddot{\mathbf{h}} + \{c_4 + (F_2 - F_1)\dot{\mathbf{j}} \sin \mathbf{j} \cos \mathbf{j}\}\dot{\mathbf{h}} \\ &= T_{1x1} \cos \mathbf{j} \cos \mathbf{y} + T_{2y2} \sin \mathbf{j} - T_{4x4} \end{aligned} \right\} \quad (1)$$

where H_0 is the spin angular momentum of G_0 , A , B , C , and E are the moments of inertia about Ox_2 , Ox_3 , Oz_4 and OX , D_1 and D_2 are the moments of inertia including G_1 and G_2 about Oz_3 and G_2 about Ox_2 , F_1 and F_2 are the moments of inertia of the G_3 about Ox_3 and Oy_3 , T_{1x1} , T_{2y2} , T_{3z3} and T_{4x4} are the torque applied about Ox_1 , Oy_2 , Oz_3 and Ox_4 , and c_1 , c_2 , c_3 and c_4 are the viscous friction coefficients about Ox_2 , Oy_3 , Oz_4 and OX , respectively.

The external torque T_{1x1} about Ox_1 supplied by the force F to the gimbal G_1 can be written as

$$\begin{aligned} T_{1x1} &= -Fa[\cos \mathbf{b} \cos \mathbf{j} \cos(\mathbf{a} + \mathbf{h}) - \sin \mathbf{b} \sin \mathbf{j} + \mathbf{q} \cos \mathbf{y} \cos \mathbf{b} \sin(\mathbf{a} + \mathbf{h}) \\ &\quad - \mathbf{q} \sin \mathbf{y} \{\cos \mathbf{b} \sin \mathbf{j} \cos(\mathbf{a} + \mathbf{h}) + \sin \mathbf{b} \cos \mathbf{j}\}] \end{aligned} \quad (2)$$

where F is the force acted on the force detector, $2a$ is the length of a lever arm. In this ideal case which means $\mathbf{a} + \mathbf{h} = 0$ and $\mathbf{b} + \mathbf{j} = 0$, rearrangement of Eq. (2) gives

$$T_{1x1} = -Fa \quad (3)$$

That is to say, from Eq. (1-1), we get the following equation, which is the principle of the GMFS,

$$H_0 \mathbf{w} = -Fa \quad (4)$$

in which the system maintains its virtually perfect linearity of the precession rate $\dot{\mathbf{u}}$ against the applied force F .

The feedback torques exerted on the G_2 , G_3 and G_4 by the torque motors are given by:

$$\begin{aligned} T_{2y2} &= k_p \mathbf{q} + k_i \int_0^t \mathbf{q} dt \\ T_{3z3} &= K_{p3}(\mathbf{j} - \mathbf{j}_r) + K_{D3}\dot{\mathbf{j}}, & T_{4x4} &= K_{p4}(\mathbf{h} - \mathbf{h}_r) + K_{D4}\dot{\mathbf{h}} \end{aligned} \quad (5)$$

where k_p and k_i are the proportional and integral gains of the torque motor installed on the G_3 , K_{p3} and K_{D3} are the proportional and derivative gains of the torque motor installed on the G_4 , K_{p4} and K_{D4} are

the proportional and derivative gains of the torque motor installed on the frame, and ζ_r and \ddot{o}_r are the reference inputs for the servomechanisms to estimate \hat{a} and $\hat{\alpha}$, respectively.

The natural frequencies and the damping coefficients of the gyroscope itself can be easily obtained by:

Low freq. mode:

High freq. mode:

$$p_1 = \sqrt{\frac{k_I}{C}}, \quad z = \frac{k_p}{2\sqrt{H_0 k_I}} \quad p_2 = \frac{H_0}{\sqrt{AB}}, \quad z = \frac{Ac_2 + Bc_1}{2H_0\sqrt{AB}} \quad (6)$$

The natural frequencies and the damping coefficients of the servomechanisms can be easily found as follows:

$$p_{s3} = \sqrt{\frac{K_{P3}}{C}}, \quad z_{s3} = \frac{K_{D3}}{2\sqrt{CK_{P3}}}, \quad p_{s4} = \sqrt{\frac{K_{P4}}{E}}, \quad z_{s4} = \frac{K_{D4}}{2\sqrt{EK_{P4}}} \quad (7)$$

Using the above characteristic values it is possible to design the GFMS, as discussed later.

2.3 Gyroscopic reaction

In order to design the servomechanisms of the G_3 and G_4 , we show the steady-state equations of the GFMS, in which PD control action is used. To find steady-state values we put $\ddot{\mathbf{y}} = 0$, $\ddot{\mathbf{q}} = \dot{\mathbf{q}} = 0$, $\dot{\mathbf{h}} = \mathbf{h} = 0$ and $\dot{\mathbf{j}} = \mathbf{j} = 0$ into Eqs. (1) through (5), and results are:

$$\left. \begin{aligned} \dot{\mathbf{y}}_e = \mathbf{w}_e = -\frac{a}{H_0} F, \quad \mathbf{q}_e = 0, \quad \mathbf{j}_e = \mathbf{j}_r + \frac{Fa \sin \mathbf{y}}{K_{P3}} \\ \mathbf{h}_e = \mathbf{h}_r - \frac{Fa \cos \mathbf{y} \cos \mathbf{j}_r}{K_{P4}} + \frac{T_{2y2} \sin \mathbf{j}_r}{K_{P4}} \end{aligned} \right\} \quad (8)$$

It should be noted that the third and fourth equations in Eq. (8) indicate additional torques due to the gyroscopic reaction. The second terms of both Eq. (8-3) and (8-4) show the oscillation components with the same frequency as that of the output \dot{u} . On the other hand, the third term of Eq. (8-4) shows the dc-component due to the integral (I) control action. These gyroscopic reaction torques can be assumed as disturbance inputs to the G_3 and G_4 . Disturbance inputs can be rejected by using a feedback compensation. By increasing the gains of compensator in servomechanisms, the sensitivity to a disturbance can be decreased.

2.4 Estimation of \hat{a} and $\hat{\alpha}$

The steady state value of the output $\dot{\mathbf{y}} = \mathbf{w}$ can be written as:

$$\mathbf{w} = -\frac{Fa}{H_0} \{ \cos \mathbf{b} \cos \mathbf{j}_r, \cos(\mathbf{a} + \mathbf{h}_r) - \sin \mathbf{b} \sin \mathbf{j}_r \} \quad (9)$$

If any three sets of reference inputs are excited as $(\mathbf{h}_{r0}, \mathbf{j}_{r0})$, $(\mathbf{h}_{r1}, \mathbf{j}_{r1})$ and $(\mathbf{h}_{r2}, \mathbf{j}_{r2})$ sequentially, the outputs \mathbf{w}_0 , \mathbf{w}_1 and \mathbf{w}_2 for each of them can be obtained by Eq. (9). The magnitudes of step-changes in the reference inputs are defined by:

$$\Delta \mathbf{h}_r = \mathbf{h}_{r1} - \mathbf{h}_{r0} = \mathbf{h}_{r2} - \mathbf{h}_{r1}, \quad \Delta \mathbf{j}_r = \mathbf{j}_{r1} - \mathbf{j}_{r0} = \mathbf{j}_{r2} - \mathbf{j}_{r1} \quad (10)$$

Initial values for $\Delta \mathbf{h}_r$ and $\Delta \mathbf{j}_r$ should be chosen to give the best estimates. Consequently, the best estimates \hat{a} and $\hat{\alpha}$ can be easily obtained.

The steady-state errors in servomechanisms are given by:

$$\mathbf{a} + \mathbf{h}_r = \mathbf{e}_a, \quad \mathbf{b} + \mathbf{j}_r = \mathbf{e}_b \quad (11)$$

where \hat{a}_a and \hat{a}_b indicate errors of estimates \hat{a} and $\hat{\alpha}$. For practical application, we can see that these errors do not influence the total amount of measuring error (less than 10^{-4}).

As a result, the components of F in three-dimensional space are given by:

$$F_x = -F \sin \mathbf{b}, \quad F_y = F \cos \mathbf{a} \cos \mathbf{b}, \quad F_z = F \sin \mathbf{a} \cos \mathbf{b}. \quad (12)$$

Based on this estimation procedure, we must determine the approximate values of the computational time Δt and the step-changes in the reference inputs $\Delta \mathbf{h}_r$ and $\Delta \mathbf{j}_r$.

3 DESIGN

The design specifications and the gain constants obtained for the GFMS are summarized in Table 1. In the feedback compensation, the criterions used in designing servomechanisms are specified to give a sufficient performance as follows:

- for the measuring error for a forcing input: measuring error 10^{-3} within a time 2 [s]
- for the disturbance suppression: magnitude ratio or gain -15 [dB]

The size and characteristics of the components of the GFMS are given in Table 2.

Table 1. Design specifications and gain constants of GFMS

	low freq.		high freq.	
natural freq.	p_1	6	p_2	70
damping coefficients	α_1	0.5	α_2	0.1
	Turntable G_3		Turntable G_4	
natural freq.	p_{s3}	24	p_{s4}	24
damping coefficients	α_{s3}	1.0	α_{s4}	1.0
gain const. of feedback loop	K_{P3} K_{D3}		K_{P4} K_{D4}	36.5 3.0

Table 2. Constants of GFMS

spin angular momentum (H_0)	0.45 [kgm ² /s]
length of lever system ($2a$)	5.5×10^{-2} [m]
moments of inertia (A)	5×10^{-3} [kgm ²]
(B)	9×10^{-3} [kgm ²]
(C)	16×10^{-3} [kgm ²]
(D)	60×10^{-3} [kgm ²]
viscous friction coefficients (C_1, C_2, C_3, C_4)	0.144 [Nms]

4 SIMULATIONS

Numerical simulations of responses to a force input were worked out to illustrate the application of the GFMS. The overall structure of the GFMS is shown by the block diagram of Fig. 2. The observed signals \mathbf{w} , \mathbf{h} and \mathbf{j} of the gyroscope and the turntables are sent to the estimator. The angles \mathbf{a} and \mathbf{b} are calculated with the estimator by itself. For the simulation, the force applied and the angles of incidence \mathbf{a} and \mathbf{b} are set to be 1 [N] and $\mathbf{a} = -45^\circ$ and $\mathbf{b} = -60^\circ$, respectively.

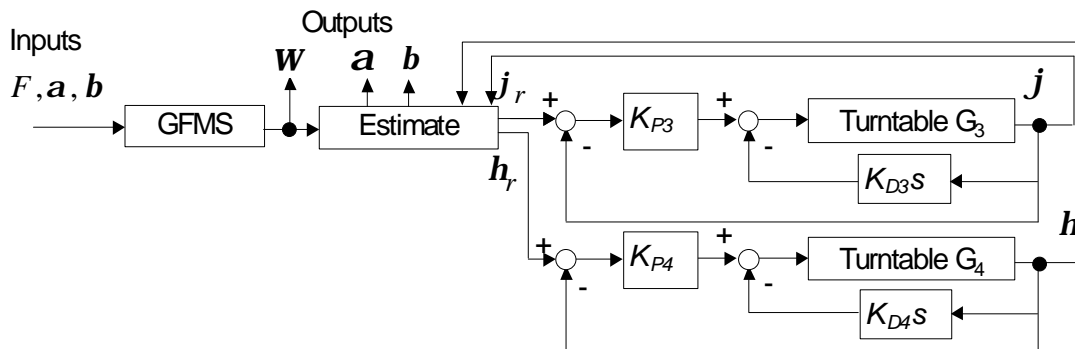


Figure 2. Overall structure of three-dimensional GMFS

Simulation results are shown in Fig. 3. The characteristic values of the GFMS are almost the same regardless of gain constants of feedback loop. The lowest diagrams show the measuring errors between the measured value (F) and the true value (F_0). It is clear from Fig. 3 that the only precession remains as the mutation is quickly damped out. Fig. 4 shows the responses of measuring errors for longer time (0 to 100 [s]). In Fig. 4, the measuring error goes through a sustained oscillation with a long period. All measuring process can be completed within 10 [s], which includes 8 [s] for to solve estimation of the angles of incidence. The estimation data are stored in a computer every 2 [s] and the procedure can be completed by two trials. Next, we demonstrate the simulated results with the estimator of \mathbf{a} and \mathbf{b} to highlight important characteristics of the GFMS. The estimator can be performed by computing the inputs \mathbf{h}_r and \mathbf{j}_r and the output \mathbf{w} as they change over a computational time Δt and step changes $\Delta \mathbf{h}_r$ and $\Delta \mathbf{j}_r$ in reference inputs. Fig. 3 shows the responses obtained, where $\Delta t = 2$ [s], $\Delta \mathbf{h}_r = \Delta \mathbf{j}_r = 20$ [deg] and $F = 1$ [N]. These simulated results show that the estimator can be successfully achieved within a time 8 [s].

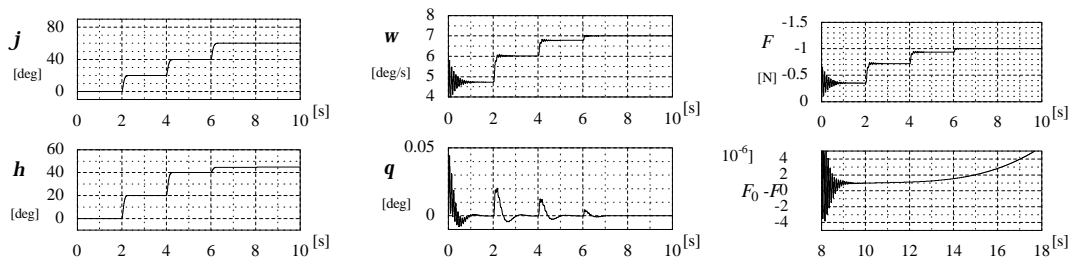


Figure 3. Responses of GFMS with PD control action

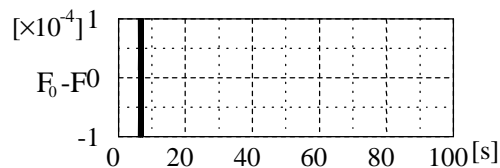


Figure 4. Sustained oscillation in error

5 CONCLUSIONS

An entirely new gyroscopic force measuring system (simply called GFMS) acts as a vectorial force sensor, which measures the magnitude and the direction of force applied externally. It is shown that the control structures and the estimator play important roles in determining the performance of the GFMS. In order to illustrate the effectiveness of the GFMS, some numerical measurement is explored, although there still remains a further engineering problem on the design and evaluation of the GFMS. The work reported here is being continued to validate conclusions obtained by experimental results.

REFERENCES

- [1] Wöhwa-Waagenbau, Josef Wöhl GmbH & Co., Postfach 7. D7114 Pfedelbach.
- [2] S. Kurosu, et. al: Dynamical characteristics of gyroscopic weight measuring device, Vol.119, *ASME Journal of Dynamic System, Measurement, and Control*, 1997, p.346-350.
- [3] H. Uchino and T. Maejima: Gyroscopic force measuring apparatus and its applications, *Instrumentation*, Vol. 25, No. 11, 1982. p. 78-84.
- [4] C. Stevens & Son Ltd.: Stevens-Wöhwa gyroscopic force measuring system, 1979.
- [5] Y. Hashimoto: Application of gyroscopic method for weighing instruments, *Technical Journal of Material Test*, Vol. 27, No. 4, 1982, p.257-267.
- [6] M. Kasahara, et. al: Analysis of gyroscopic sensor applied to force measurement ----vectorial measurement of horizontal force----, *Proceedings of the IMECO TC3/APMF'98*, Taejon Korea, 1998, p. 128-136.

AUTHORS: Prof. Dr. Shigeru KUROSU, Ass. Masato KASAHARA and Student Kazuhiro KODAMA, Oyama National College of Technology, 771 Nakakuki, Oyama-city, 323-0806 Japan, Phone Int. and Fax Int. +81-285-21-0302, E-mail: kurosu@oyama-ct.ac.jp